Journal of Alloys and Compounds 293–295 (1999) 862–867

Effect of the disproportionation and recombination stages of the HDDR process on the inducement of anisotropy in Nd–Fe–B magnets

S. Sugimoto*, H. Nakamura, K. Kato, D. Book, T. Kagotani, M. Okada, M. Homma

Department of Materials Science, Graduate School of Engineering, Tohoku University, Aoba-yama 02, Sendai 980-8579, Japan

Abstract

The magnetic properties of HDDR (hydrogenation disproportionation desorption recombination) treated $Nd_{12.2}Fe_{81.8}B_{6.0}$ alloys were investigated. Two different patterns were used for the disproportionation stage: (i) the alloys were heated to a certain processing temperature between 850–950°C in 0.1 MPa of hydrogen (conventional hydrogen treatment: *c-HD* treatment), and (ii) the alloys were heated under vacuum and hydrogen was only admitted when the processing temperature had been reached (*ν-HD* treatment). The alloys were then held at the processing temperature for 1 or 2 h under hydrogen in order to cause complete disproportionation. Either an argon heat treatment, or a hydrogen heat treatment at various constant pressures below 0.1 MPa, was then used to control the hydrogen pressure during the recombination stage (*s-DR* treatment), followed by the usual heat treatment in vacuum (conventional heat treatment in vacuum: *c-DR* treatment) to cause complete recombination. It was found that the magnetic properties of the *ν*-HD powders were more sensitive to the *s*-DR treatment time than those of the *c*-HD powders, which is thought to be related to differences in microstructure observed in the disproportionated state. The best magnetic properties were obtained for a *ν*-HD powder *s*-DR treated at 950°C for 20 min: B_r=1.4 T, $_jH_c$=385 kAm^{-1}, B_r/J_s=0.92. It can be said that the inducement of anisotropy is influenced by the hydrogenation and desorption stages of the HDDR process, and that the combination of *ν*-HD and *s*-DR treatment can be an effective method of inducing anisotropy in Nd–Fe–B powders.

Keywords: Nd–Fe–B; HDDR; Anisotropy; Disproportionation; Recombination; Hydrogen pressure

1. Introduction

The hydrogenation, disproportionation, desorption, and recombination (HDDR) phenomena in Nd–Fe–B alloys [1,2] occur after a heat treatment in hydrogen, and a subsequent heat treatment under vacuum. Nd–Fe–B powders produced by utilizing the HDDR phenomena are useful for the production of high performance anisotropic bonded magnets [3].

While it has been shown that the addition of Co, Ga, Zr or Nb can induce magnetic anisotropy in HDDR treated magnets [3], an investigation of hydrogen absorption and desorption characteristics [4], and resistivity measurements during HDDR phenomena [5] in our previous works suggested that the main effect of additives is to alter the HDDR conditions. In addition, the authors have shown that anisotropic powders can be prepared from the ternary alloy, by raising the vacuum treatment temperature to higher than 800°C [6]. These results show that not only additives, but also the treatment conditions are important in obtaining anisotropic powder. However, the most suitable HDDR treatment conditions for the enhancement of magnetic anisotropy have not yet been established, because the mechanism for the induction of anisotropy during HDDR is still not understood.

Recently, a study into the effect of HDDR conditions on the ternary alloy was carried out, and the temperature dependence of the recombination pressure of the $Nd_2Fe_{14}B$ compound was clarified, as shown in Fig. 1 [7]. The pressure–temperature plot can be divided into three regions: (I) in which the $Nd_2Fe_{14}B$ compound is stable; (II) in which the disproportionated mixture is stable; (III) in which, although the disproportionated mixture is more stable, the $Nd_2Fe_{14}B$ compound (or its hydride) exists because of unfavourable kinetics at these low temperatures. Using this result, it may be possible to discover the HDDR conditions necessary for the enhancement of magnetic anisotropy. Therefore, the aim of this study is to investigate the magnetic properties of HDDR treated Nd–

---

*Corresponding author.

0925-8388/99/$ – see front matter
PII: S0925-8388(99)00376-X

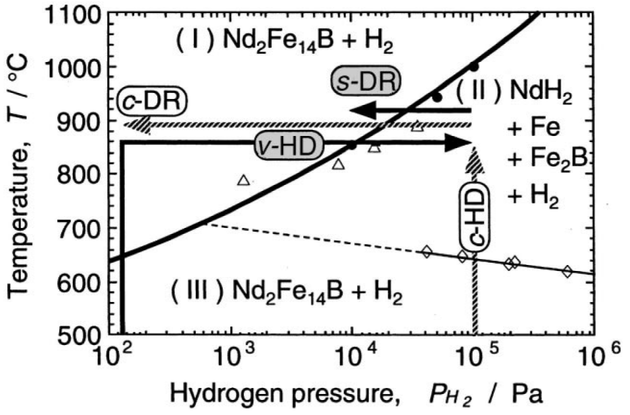

Fig. 1. The hydrogen pressure–temperature curve of the recombination reaction of the $Nd_2Fe_{14}B$ compound, and the starting disproportionation reaction during heating. (After [7] which includes data from [5,8,9].) The *c*-HD and *v*-HD denote the routes of conventional and new treatments for disproportionation reaction, respectively. The *c*-DR and *s*-DR also exhibit the routes of those treatments for recombination reaction.

Fe–B powders under treatment conditions that were selected using data from Fig. 1.

2. Experimental procedures

The composition of the studied alloys was $Nd_{12.2}Fe_{81.8}B_{6.0}$. The alloy specimens were induction melted using high purity elements and ferroalloys, under an Ar atmosphere, and were then homogenized at 1150°C for 50 h.

The HDDR treatment was carried out on hydrogen decrepitated ingots. In Fig. 1, Nd–Fe–B alloys go from (III)→(II)→(I) in the conventional HDDR process [1]. However, under suitable conditions, the route (I)→(II)→(I) should also be possible. Two types of treatments were chosen for the disproportionation stage: (i) the samples were heated in $P_{H_2}=0.1$ MPa at a rate of 400°C h^{-1} up to 850–950°C and then held at this temperature for 2 h, we have referred to this as the '*c*-HD treatment' (*c*onventional *H*ydrogenation *D*isproportionation) (the route (III)→(II)), and (ii) the samples were heated under vacuum up to a treatment temperature between 850–950°C, exposed to a mixture of hydrogen and Ar ($P_{H_2}\leq0.1$ MPa) for 1 h and then exposed to 0.1 MPa of hydrogen for a further 1 h, we have referred to this as the '*ν*-HD treatment' (heating in *v*acuum then *H*ydrogenation *D*isproportionation) (the route (I)→(II)).

For the recombination stage, a heat treatment was used in which Ar was flushed through the system before the usual evacuation treatment, using a rotary pump. Since the rate of the recombination reaction was relatively slow during Ar flushing, compared to the usual evacuation treatment, we have referred to the Ar heat treatment as the '*s*-DR treatment' (*s*low *D*esorption *R*ecombination), and to the conventional evacuation treatment as the '*c*-DR treatment' (*c*onventional *D*esorption *R*ecombination). The *s*-DR and *c*-DR treatments were performed at the same temperature as the treatment in the recombination stage. The *s*-DR treatment time was varied from 0 (i.e. no *s*-DR treatment) to 90 min. However, the *c*-DR treatment time was not fixed, but rather the pressure of the rotary pump was monitored, and when the recombination reaction was observed to finish, the samples were rapidly cooled. In addition to the Ar flushing treatment, another type of *s*-DR treatment was tried. In this treatment, a constant pressure of hydrogen (100–2600 Pa) was maintained by monitoring the pressure of the sample while it desorbed hydrogen and adjusting the pressure with a needle valve. The combination of *c*-HD and *c*-DR treatments is the typical HDDR treatment condition and may be called conventional HDDR [1,2]. The combination of *v*-HD and *c*-DR is similar to 'solid-HDDR' [10], which has been used to obtain solid samples by avoiding hydrogen decrepitation. However, in this work hydrogen decrepitated powders were used, and the purpose of the initial heating in vacuum is to change the disproportionated microstructure and thereby affect the final magnetic properties of the recombined material.

HDDR treated ingots were ground into powders of <63 mm by milling. 50 mg samples of these powders were mixed with molten paraffin in a cylindrical case (internal diameter=6 mm, and internal height=3 mm), and the paraffin was allowed to solidify in a magnetic field of 960 kAm^{-1} which was applied parallel to the bottom of the case. The magnetic properties were measured using a vibrating sample magnetometer (VSM) with a maximum applied field of 1.2 MAm^{-1}, after applying a pulsed field of 4.0 MAm^{-1} to the sample. The density of the homogenized ingots, and a demagnetizing factor of 0.12 which was determined by measuring the as-homogenized powder, were used for the VSM measurements. The microstructures of the ingots were observed using an optical microscope and a field emission scanning electron microscope (FE-SEM).

3. Results and discussions

Fig. 2 shows the remanence (B_r) and coercivity ($_jH_c$) of $Nd_{12.2}Fe_{81.8}B_{6.0}$ alloy specimens disproportionated by either the (a) *c*-HD treatment, or (b) *v*-HD treatment, and subsequently recombined by the *c*-DR treatment. The normalized remanence (B_r/J_s), which was calculated using the magnetization intensity of aligned as-homogenized powder (J_s), is indicated by a dashed line for the value 0.5. The coercivities of the *c*-HD and *v*-HD treated samples exhibited maximum values of around 0.9 MAm^{-1} between 850 and 900°C. However, the remanence values had different temperature dependencies: the remanence of the *v*-HD samples decreased with increasing heat treatment temperature, while that of the *c*-HD samples increased

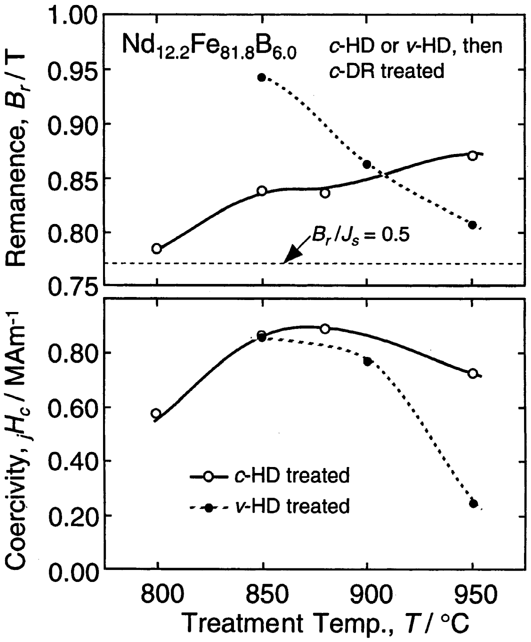

Fig. 2. Remanence (B_r) and coercivity ($_jH_c$) of $Nd_{12.2}Fe_{81.8}B_{6.0}$ alloys disproportionated by either the (a) *c*-HD treatment, or (b) *v*-HD treatment and subsequently recombined by *c*-DR treatment.

monotonically. The *v*-HD sample treated at 850°C exhibited the highest remanence of 0.94 T with a B_r/J_s value of 0.61. The large difference in remanence between the *v*-HD and *c*-HD samples, may be ascribed to the differences in microstructure after disproportionation.

Fig. 3 shows optical and SEM microstructures of $Nd_{12.2}Fe_{81.8}B_{6.0}$ after *c*-HD ((a) and (b)) and *v*-HD ((c) and (d)) treatments at 950°C. The optical micrograph of Fig. 3 (a) shows that the *c*-HD sample has a relatively uniform microstructure consisting of disproportionated mixture. In the SEM micrograph shown in Fig. 3 (b), spherical NdH_2 grains of less than 1 μm in diameter (denoted by 'S'), embedded in an Fe matrix ('M') were observed, together with fine NdH_2 grains ('R'). This morphology is characteristic of the disproportionated mixture [11,12]. The optical micrograph shown in Fig. 3 (c) reveals that the *v*-HD treatment results in quite a different morphology. Coarse lamellae ('C') form a network, and fine lamellae with an inter-lamellar spacing of about 250 nm (as shown by the close up of area 'F' in Fig. 3 (d)), can be observed inside this network. Similar microstructures have been reported by Gutfleisch et al. [10] and Gao et al. [13]. The samples *v*-HD treated at 850°C had morphologies similar to those treated at 950°C, however, the lamellar spacing was significantly smaller.

Fig. 4 is a schematic illustration of the microstructural changes that occur during the disproportionation reaction for the *c*-HD and *v*-HD treatments. In the *c*-HD sample, the disproportionation reaction first takes place near the grain boundaries and hydrogen diffuses into grains during heating in hydrogen, resulting in a uniform distribution of fine lamellae forming at the boundary of (III) and (II) in Fig. 1. The disproportionation reaction is accompanied by a large volume expansion and it is possible that the disproportionated mixture prefers to form a lamellar structure in order to reduce the strain due to the volume change. However, this results in a large interfacial energy and the lamellae will then grow, with increasing temperature, to form spherical grains of NdH_2 in order to reduce the interfacial energy. The disproportionation reaction during *v*-HD treatment is also considered to begin at grain

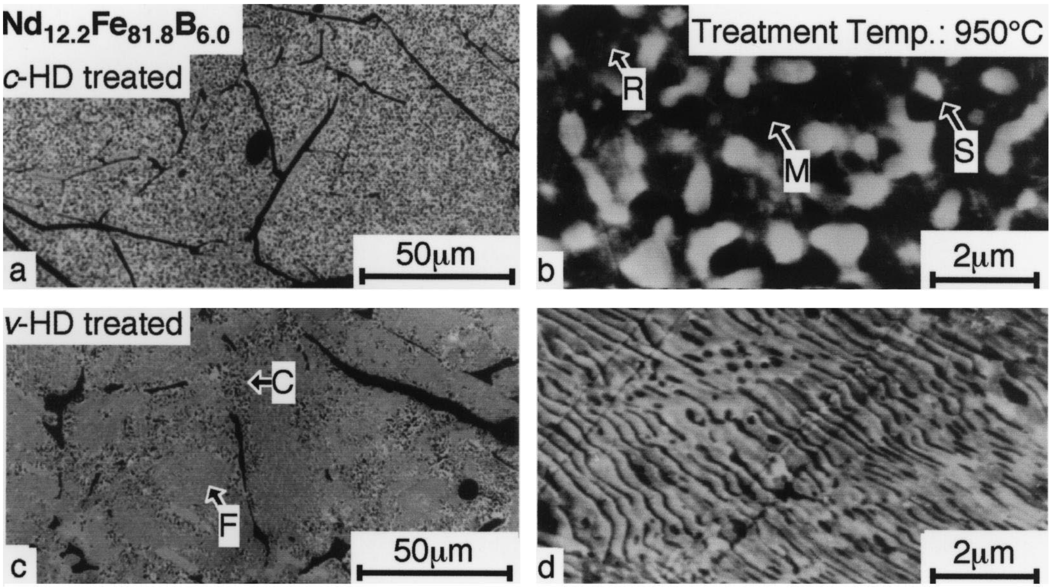

Fig. 3. Microstructures of $Nd_{12.2}Fe_{81.8}B_{6.0}$ after disproportionation at 950°C. *c*-HD treatment: (a) optical microscope image, and (b) FE-SEM image. (Regions of NdH_2 (S and R) and Fe (M) are labelled.) *v*-HD treatment: (c) optical microscope image showing fine and coarse lamellae regions, denoted by F and C, respectively, and (d) FE-SEM image of a close-up of region F.

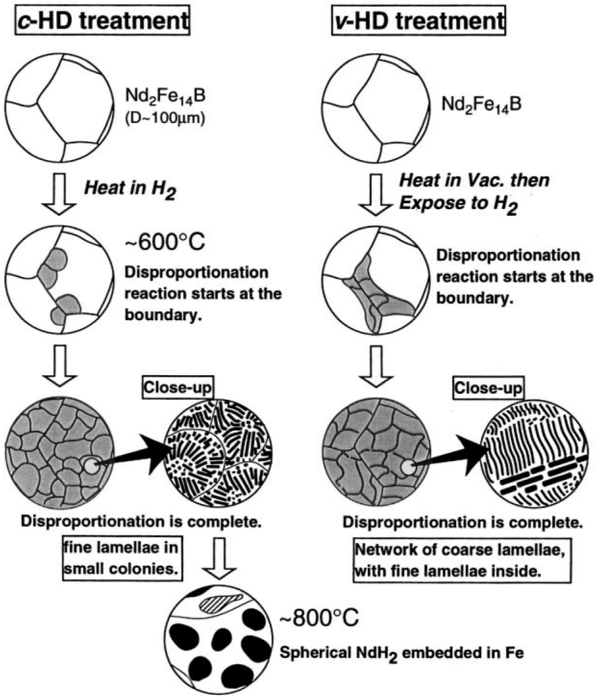

Fig. 4. Schematic illustration of microstructural changes during the disproportionation reaction for the *c*-HD and *v*-HD treatments.

boundaries. However because of the higher treatment temperature, hydrogen diffusion into the grains and growth of the fine lamellae occurs almost simultaneously, which leads to a more inhomogeneous morphology than for *c*-HD treated samples. In addition, the coarse lamellae form a network which may act as a diffusion path for hydrogen at the early stage of the reaction.

Accordingly, it may be said that the state of the disproportionated mixture is the key to the inducement of anisotropy during HDDR, and that the fine lamellar structure, rather than the spherical structure, results in highly oriented $Nd_2Fe_{14}B$ grains after recombination. These two different kinds of disproportionation process were then used to investigate the effect of the recombination stage.

Fig. 5 shows the remanence (B_r) and coercivity ($_jH_c$) of $Nd_{12.2}Fe_{81.8}B_{6.0}$ alloys after HDDR treatment at 850 and 950°C, vs. *s*-DR treatment time. The samples were disproportionated by either the (a) *c*-HD treatment, or (b) *v*-HD treatment. Normalized remanence (B_r/J_s), is indicated by dashed lines for the values 0.5 and 1.0. The $t=0$ min samples had no *s*-DR treatment, and so were only processed with the *c*-DR treatment. In the samples disproportionated by *c*-HD treatment at 850°C, the remanence increases gradually from 0.85 to 1.0 T with increasing *s*-DR treatment time. With a treatment temperature of 950°C, the remanence was higher up to an *s*-DR treatment time of about 40 min. The coercivities were not very sensitive to *s*-DR treatment time under these conditions. In contrast to the *c*-HD treated samples, the *v*-HD samples exhibited greatly enhanced remanence due to the *s*-DR treatment, as shown in Fig. 5 (b). A maximum value of 1.4 T ($B_r/J_s=0.92$) was obtained for the sample HDDR treated at 950°C with an *s*-DR treatment of 20 min. Therefore, it may be said that the *s*-DR treatment is an effective method of producing highly anisotropic Nd–Fe–B HDDR powders, and that the conditions during the disproportionation stage also affect the inducement of anisotropy.

This *s*-DR treatment has in fact been used in our laboratory for the HDDR processing of the $Nd_2Fe_{14}B$ compound [6]. Recently, Nakayama et al. [14] reported similar results in which annealing under an Ar atmosphere before the evacuation treatment, was found to enhance the remanence of HDDR treated Nd–Dy–Fe–Co–B–Ga–Zr powders, although the standard *c*-HD treatment was used for the disproportionation stage.

The hydrogen pressure during the recombination stage by *c*-DR and *s*-DR was monitored, which showed that the hydrogen pressure during the *s*-DR treatment is higher than that during the *c*-DR treatment. This results in a very

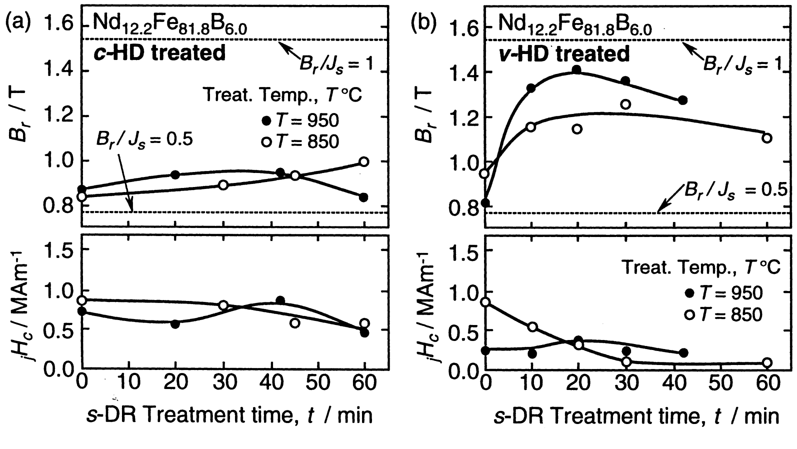

Fig. 5. Remanence and coercivity of $Nd_{12.2}Fe_{81.8}B_{6.0}$ alloys after HDDR treatment at 850 and 950°C vs. *s*-DR treatment time, for samples that had been disproportionated by the (a) *c*-HD, and (b) *v*-HD treatment.

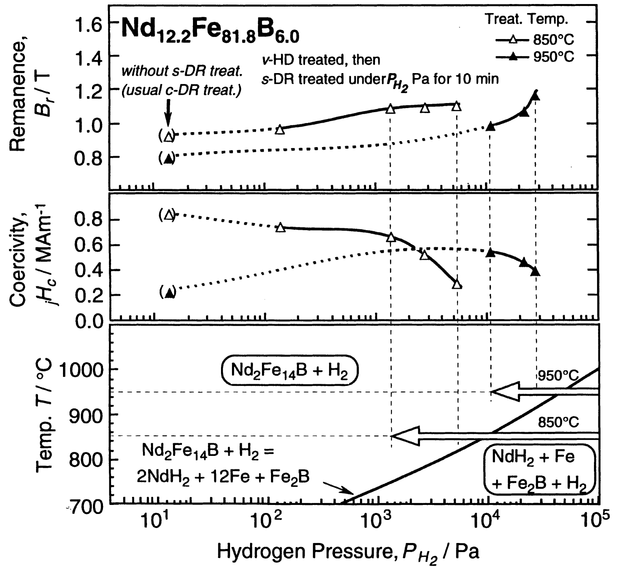

Fig. 6. Remanence and coercivity of v-HD treated $Nd_{12.2}Fe_{81.8}B_{6.0}$ alloys after s-DR treatment at 850 and 950°C for 10 min, against P_{H_2}.

large difference in the reaction time of recombination, with the c-DR treatment taking less than 3 min to reach completion, and the s-DR treatment taking more than 20 min. It can be said that the Ar-flushing version of the s-DR treatment controls the hydrogen pressure in the early stage of the recombination reaction. However, the Ar-flushing treatment includes many parameters which are difficult to quantify or control. Therefore, another s-DR treatment was tried in which the hydrogen pressure was maintained at a constant pressure by continuously adjusting the pressure with a needle valve.

Fig. 6 shows the remanence and coercivity of v-HD treated $Nd_{12.2}Fe_{81.8}B_{6.0}$ alloys after this type of s-DR treatment, at 850 and 950°C for 10 min, against P_{H_2}. Also shown is the pressure–temperature curve for the recombination reaction of the $Nd_2Fe_{14}B$ compound. Remanence increased with increasing P_{H_2}, and results similar to those for the Ar flushing treatment (Fig. 5) were obtained. A similar result for Nd–Fe–B–Ga alloys was reported by Gao et al. [15]. Comparing these data with the pressure–temperature curve, it can be seen that a higher remanence is obtained at hydrogen pressures close to the recombination pressure of the $Nd_2Fe_{14}B$ compound.

Fig. 7 shows a schematic illustration of the microstructure due to the difference in hydrogen pressure during the recombination reaction. From the results described above, it may be said that the hydrogen pressure during the recombination stage P_{H_2} has an associated free energy change ΔG, which will affect the driving force of the recombination reaction and the frequency of nucleation of the newly formed $Nd_2Fe_{14}B$ grains. The value of ΔG will increase with decreasing P_{H_2}, below the recombination pressure–temperature line of the $Nd_2Fe_{14}B$ compound. Assuming that the nucleation of $Nd_2Fe_{14}B$ grains with the same orientation as the original grains requires only a small free energy change, then the enhancement in anisotropy after the s-DR treatment could be explained by the higher hydrogen pressure ($P_{H_2} > P_2$). In contrast, a lower hydrogen pressure ($P_{H_2} < P_2$) would result in a larger free energy change, and therefore the formation of a greater number of misoriented nuclei.

To conclude, the combination of v-HD and s-DR treatments is an effective way of obtaining highly anisotropic Nd–Fe–B HDDR powders.

Acknowledgements

The authors would like to thank Mr. H. Murai and Mr. T. Kobayashi for their assistance in many experiments. This work has been supported in part by a Grant-in-Aid for

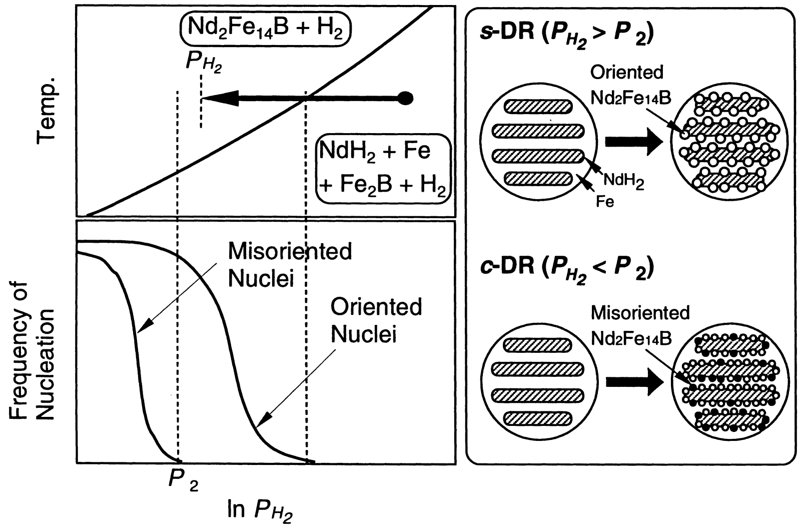

Fig. 7. Schematic illustration of the microstructure due to the difference in hydrogen pressure during the recombination reaction.

Scientific Research on Priority Areas A of ‘New Protium Function’ and No. 10450252 from the Ministry of Education, Science, Sports and Culture of Japan.

References

[1] T. Takeshita, R. Nakayama, Proc. 10th Int. Workshop on R. E. Magnets & Their Applications, Kyoto, 1989, p. 551.

[2] P.J. McGuiness, X.J. Zhang, X.J. Yin, I.R. Harris, J. Less-Common Met. 158 (1990) 359.

[3] T. Takeshita, R. Nakayama, Proc. 12th Int. Workshop on R. E. Magnets & Their Applications, Canberra, 1992, p. 670.

[4] H. Nakamura, S. Sugimoto, T. Tanaka, M. Okada, M. Homma, J. Alloys Comp. 222 (1995) 136.

[5] S. Sugimoto, O. Gutfleisch, I.R. Harris, J. Alloys Comp. 260 (1997) 284.

[6] H. Nakamura, R. Suefuji, S. Sugimoto, M. Okada, M. Homma, J. Appl. Phys. 76 (1994) 6828.

[7] H. Nakamura, K. Kato, D. Book, S. Sugimoto, M. Okada, M. Homma, Proc. 15th Int. Workshop on R. E. Magnets & Their Applications, Dresden, 1998, p. 507.

[8] W.L. Korst, J.C. Warf, Inorg. Chem. 5 (1966) 1719.

[9] D. Book, I.R. Harris, J. Alloys Comp. 221 (1995) 187.

[10] O. Gutfleisch, M. Matzinger, J. Fidler, I.R. Harris, J. Magn. Magn. Mater. 147 (1995) 320.

[11] H. Nakamura, R. Suefuji, D. Book, T. Kagotani, S. Sugimoto, M. Okada, M. Homma, Mater. Trans., JIM 37 (1996) 482.

[12] M. Itakura, N. Kuwano, K. Yamaguchi, T. Yoneki, K. Oki, R. Nakayama, N. Komada, T. Takeshita, Mater. Trans., JIM 39 (1998) 95.

[13] J. Gao, X. Song, X. Wang, J. Alloys Comp. 248 (1997) 176.

[14] R. Nakayama, Y. Ishii, K. Morimoto:, J. Magn. Soc. Jpn 22 (1998) 361, (in Japanese).

[15] J. Gao, X. Song, X. Wang, J. Alloys Comp. 267 (1998) 270.